INVESTIGATION OF THE TEMPERATURE REGIMES OF BODIES IMMERSED IN FLOW WITH SURFACE BLOWING

V. I. Zinchenko, A. G. Kataev, and A. S. Yakimov

UDC 533.526-536.24

For a body immersed in a high-enthalpy stream the flow of heat along generators can be an efficient method of lowering the surface temperature for regions of maximum heat flux, as has been shown for steady conditions in [1, 2]. Another method of thermal protection of structures is blowing of coolant gas, which reduces the surface heat flux, and where heat is rejected during filtering in the pores. There is interest in investigating the simultaneous action of these factors on the distribution of temperature in the gas and condensed phases and of the heat flux to the surface of the immersed body.

This paper examines the solution of the heating problem in supersonic flow over a blunted sphere-cone, allowing for different flow regimes in the boundary layer and surface blowing of gas from the spherical region. We shall study the influence of the flow regimes and the mass flux of blown gas, the body geometry, and the thermophysical properties of the material on the characteristics of the unsteady coupled heat and mass transfer.

1. In accordance with [3, 4] we shall seek the characteristics of the coupled heat and mass transfer by solving the system of equations describing the variation of mean values of quantities in the boundary layer, the energy conservation equation for the porous spherical part of the body, and the unsteady heat conduction equation for the conical part.

In terms of Dorodnitsyn–Lees variables for the gas phase in the natural coordinate system fixed in the outer body surface, the system of equations in dimensionless variables has the form

$$\frac{\partial}{\partial\eta}\left(l\frac{\partial\bar{u}}{\partial\eta}\right)+f\frac{\partial\bar{u}}{\partial\eta}=\alpha\left(\bar{u}\frac{\partial\bar{u}}{\partial\xi}-\frac{\partial f}{\partial\xi}\frac{\partial\bar{u}}{\partial\eta}\right)+\beta\left(\bar{u}^2-\frac{\rho_e}{\rho}\right); \tag{1.1}$$

$$\frac{\partial}{\partial\eta}\left[\frac{l}{\mathrm{Pr}_\Sigma}\frac{\partial g}{\partial\eta}+\frac{u_e^2}{H_e}l\left(1-\frac{1}{\mathrm{Pr}_\Sigma}\right)\bar{u}\frac{\partial\bar{u}}{\partial\eta}\right]+f\frac{\partial g}{\partial\eta}=\alpha\left(\bar{u}\frac{\partial g}{\partial\xi}-\frac{\partial f}{\partial\xi}\frac{\partial g}{\partial\eta}\right). \tag{1.2}$$

For the porous spherical surface ($0 \le \xi \le \xi_1$), assuming the process of filtering the blown gas is one-dimensional in the direction normal to the surface, we have

$$\pi_{\rho_1}\frac{\partial\theta}{\partial\tau}=\frac{1}{H_1 r}\left[\frac{\partial}{\partial\xi}\left(\frac{r}{H_1}\pi_{\lambda_1}\frac{\partial\theta}{\partial\xi}\right)+\frac{\partial}{\partial n_1}\left(rH_1\pi_{\lambda_1}\frac{\partial\theta}{\partial n_1}\right)\right]+(\overline{\rho v})_w\frac{\sqrt{\mathrm{Re}}\,\mathrm{Pr}\,\lambda_{e0}}{\lambda_*}\frac{r_w}{rH_1}\frac{\partial\theta}{\partial n_1}. \tag{1.3}$$

For the conical part of the body we have

$$\pi_{\rho_2}\frac{\partial\theta}{\partial\tau}=\frac{1}{r}\left[\frac{\partial}{\partial\xi}\left(r\pi_{\lambda_2}\frac{\partial\theta}{\partial\xi}\right)+\frac{\partial}{\partial n_1}\left(r\pi_{\lambda_2}\frac{\partial\theta}{\partial n_1}\right)\right]. \tag{1.4}$$

We write the boundary and initial conditions as

$$\bar{u}(\xi,\infty)=g(\xi,\infty)=1; \tag{1.5}$$

$$\bar{u}(\xi,0)=0,\quad f(0,\xi)=f_w=\frac{\int\limits_0^\xi(\overline{\rho v})_w r_w d\xi}{\left(2\int\limits_0^\xi\frac{\rho_e}{\rho_{e0}}\frac{\mu_e}{\mu_{e0}}\frac{u_e}{v_m}r_w^2 d\xi\right)^{0.5}}, \tag{1.6}$$

Tomsk. Translated from Prikladnaya Mekhanika i Tekhnicheskaya Fizika, No. 6, pp. 57-64, November-December, 1992. Original article submitted June 19, 1991; revision submitted September 27, 1991.

0021-8944/92/3306-0821$12.50

$$\tilde{q}_w(\xi,0)\sqrt{\mathrm{Re}}\,\mathrm{Pr}\frac{\lambda_{e0}}{\lambda_*}-\pi_\sigma\theta_w^4=-\left(\pi_{\lambda i}\frac{\partial\theta}{\partial n_1}\right)_w,\quad i=1,2;$$

$$\left(\pi_{\lambda_1}\frac{\partial\theta}{\partial n_1}\right)\Big|_{w1}=\sqrt{\mathrm{Re}}\,\mathrm{Pr}\frac{\lambda_{e0}}{\lambda_*}\frac{r_w}{(rH_1)_{w1}}(\overline{\rho v})_w(\theta_i-\theta_{w1})\quad\text{for}\quad 0\leqslant\xi\leqslant\xi_1,\tag{1.7}$$

$$\frac{\partial\theta}{\partial n_1}\Big|_{w1}=0,\quad \xi>\xi_1;$$

$$\frac{\partial\theta}{\partial\xi}\Big|_{\xi=0}=0,\quad \frac{\pi_{\lambda_1}}{H_1}\frac{\partial\theta}{\partial\xi}\Big|_{\xi=\xi_1}=\pi_{\lambda_2}\frac{\partial\theta}{\partial\xi}\Big|_{\xi=\xi_1},\quad \frac{\partial\theta}{\partial\xi}\Big|_{\xi=\xi_K}=0;\tag{1.8}$$

$$\theta(0,\ \xi,\ n_1)=\theta_i,\ 0\leqslant\xi\leqslant\xi_K.\tag{1.9}$$

Here $\bar{u}=u/u_e$, $g=H/H_e$, $\theta=T/T_{e0}$ are, respectively the dimensionless velocity, the total enthalpy and the surface temperature; n_1 is a coordinate referenced to the blunting radius R_N; $\alpha=2\int_0^\xi\rho_e\mu_eu_er_w^2d\xi/(\rho_e\mu_eu_er_w)^2$; $\beta=\frac{\alpha}{u_e}\frac{du_e}{d\xi}$; $H_1=1-n_1$, $r=r_w-n_1\cos\alpha$ are Lamé coefficients; $(\overline{\rho v})_w=\frac{(\rho v)_w\sqrt{\mathrm{Re}}}{\rho_{e0}v_m}$ is the dimensionless mass flow rate of coolant gas; and $\pi_{\rho_1}=\frac{\rho_1c_1}{\rho_*c_*}\times(1-\varphi)+\frac{\rho_gc_{pg}}{\rho_*c_*}\varphi$; $\pi_{\rho_2}=\frac{\rho_2c_2}{\rho_*c_*}$; $\pi_{\lambda_1}=\frac{\lambda_1}{\lambda_*}(1-\varphi)+\frac{\lambda g}{\lambda_*}\varphi$; $\pi_{\lambda_2}=\frac{\lambda_2}{\lambda_*}$; $\mathrm{Re}=\frac{\rho_{e0}v_mR_N}{\mu_{e0}}$; $\pi_\sigma=\frac{\varepsilon\sigma T_{e0}^3R_N}{\lambda_*}$; $\tau=\frac{t}{t_*}$; $t_*=\frac{R_N\rho_*c_*}{\lambda_*}$ is the characteristic time. In the general case of transition of laminar boundary layer flow to turbulent we have

$$l=\rho(\mu+\Gamma\mu_T)/\rho_e\mu_e,\quad \mathrm{Pr}_\Sigma=\frac{(\mu+\Gamma\mu_T)\,\mathrm{Pr}\mathrm{Pr}_T}{\mu\,\mathrm{Pr}_T+\Gamma\mu_T\,\mathrm{Pr}}.$$

In Eq. (1.6) the dimensionless flux $\tilde{q}_w(\xi,0)$ is linked to the dimensions as follows: $\tilde{q}_w=\frac{\mu_w}{\mathrm{Pr}}\frac{\partial H}{\partial n}\Big|_w\frac{\sqrt{\mathrm{Re}}}{\rho_{e0}v_mH_e}$. The subscripts e, e0, and w refer to values at the outer edge of the boundary layer, at the outer edge at the stagnation point, and on the boundary surface $n_1=0$, respectively; w1 refers to conditons on the inside of the body wall of thickness L/R_N; 1 and 2 refer to the characteristics of the condensed phase on the spherical and conical parts; * to characteristics of the material; g to the gas phase of the porous spherical shell; and T and i to characteristics of turbulent transfer and initial conditions.

To describe the turbulent flow we apply the two-layer turbulent boundary layer model [5]. In the inner region the turbulent viscosity is found from the Prandtl formula with the Van Driest–Sebeci damping factor, accounting for the pressure gradient and the surface blowing. In the outer region we use the Clauser formula. The longitudinal mixing length G was taken from [6]. A detailed account of the turbulence model used has been given in [7], where the authors compared theory and experiment, confirming that this turbulent model may be used. We note that at the computed Reynolds numbers the heat flux data coincide for both models of the turbulent viscous shock layer and boundary layer.

As follows from the statement of the problem, the governing parameters are the body geometry, the Mach number M_∞ and the Reynolds numbers Re, γ, the initial temperature θ_w and the dimensionless mass flow rate law $(\overline{\rho v})_w(\xi)$. For constant and identical thermophysical characteristics of the material of the porous blunted and the conical sections, to the above we add parameters describing the heat and mass fluxes to and from the body: the matching parameter $S=\sqrt{\mathrm{Re}}\,\mathrm{Pr}\,\lambda_{e0}/\lambda_*$, defining the ratio of convective to conduction heat flux, the parameter π_σ expressing the ratio of the radiative to conduction heat flux, and the relative wall thickness α/R_N.

In the numerical integration we took Pr = 0.72, $\mathrm{Pr}_T=1$, and the molecular viscosity was found from the Sutherland law. The numerical integration of the boundary layer system of equations was carried out with a difference scheme obtained with the aid of the iteration-interpolation method of [8]. The two-dimensional equations (1.3) and (1.4) were computed by the splitting method of [9], combined with the method of [8]. For the turbulent flow in the boundary layer we developed combined difference shcemes, matching the desired characteristics in the laminar sublayer and the turbulent core, and accounting for the variation of μ_T across the boundary layer. This allowed us to increase the rate of convergence of the iteration process and to carry through the computations for any values of Re at various values of the flow rate of blown gas from the body surface.

2. We now consider the results of solving the boundary problem of Eq. (1.1)-(1.9). We computed the flow over a spherically blunted cone of semi-opening angle 5° for governing parameters corresponding to the wind tunnel test conditions. The model geometry, the stagnation point pressure, and the law of blown gas flow rate from the blunted surface corresponded to the data of [10]: $M_\infty = 5$, $R_N = 0.0508$ m, $p_{e0} = 3.125 \cdot 10^5$ N/m², $(\rho v)_w(\xi) = \mathrm{const} = 1.626$ kg/(m²·sec). The computations, performed for $T_{e0} = 525$ K for conditions corresponding to an initial isothermal wall temperature of $T_w = T_i = 288$ K, showed satisfactory agreement between the theory and the experimental results [7]. In this case, to investigate the unsteady heating process T_{e0} was assumed to be 1500 K, the thermophysical properties of the wall material were assumed to be constant, the wall was assumed to be made of copper, a good conductor, and the nonconducting wall was assumed to have the properties of asbestos. The emissivity was taken as $\varepsilon = 0.7$, the basic computations were performed for a thin wall ($L/R_N = 0.0425$), for which the maximum temperature was reached.

Figure 1 shows, for the laminar flow case, the distribution of heat flux and surface temperature for flow over an inpermeable thin wall (solid curves) and with blowing (broken curves) at different times. Lines 1-3 correspond to material with high thermal conductivity (S = 0.15) at times t = 0, 30, 210 sec, and curves 1'-3' were obtained for a nonconducting wall (S = 470) for t = 0, 1, 60 sec. Curves 1 and 1' coincide at the initial time for T_i = 288 K. The computations were made until the end of the steady-state regime of the process and additional autonomous calculations were made of the boundary problem of determining the equilibrium radiative surface temperature T_{wp} shown by dot-dash lines in Fig. 1. In this case for $(\rho v)_w = 0$ we have

$$\tilde{q}_w(\xi, 0)\, S = \pi_\sigma \theta_{wp}^4, \tag{2.1}$$

and with blowing on the spherically blunted surface the energy conservation condition was taken, allowing for the steady solution for a thin porous wall

$$\tilde{q}_w(\xi, 0) = \frac{\pi_\sigma}{S}\theta_{wp}^4 + \overline{(\rho v)}_w'(\theta_{wp} - \theta_i). \tag{2.2}$$

We note that in solving the coupled problem for a thermally insulating material curves 3' coincide with values of the radiative equilibrium temperature T_{wp}. As follows from Fig. 1, for $(\rho v)_w = 0$ the reduction of the maximum temperature T_w in the vicinity of the stagnation point when using the heat conducting material is about 100 K, due to the flow of heat from the blunted region to the conical section and subsequent radiation from the surface. An increase of wall thickness by a factor of 2 (dotted lines, obtained for t = 500 sec at the end of the steady-state regime) leads to a decrease of $T_w(0)$ by 50 K more, and thus, by a choice of L/R_N we can control the amount of decrease of wall temperature in the blunted region. On the conical part of the surface for the conducting material T_w is negligibly greater than the corresponding value T_{wp}. The substantial decrease of wall temperature is achieved for the nominal blowing through the permeable blunting. A thermal curtain regime is achieved behind the blowing section and the maximum wall temperatures are reached on the conical surface. The use of heat conducting material also leads to equilibration of the wall temperature, and here the heat flow occurs towards the spherically blunted section and on the peripheral part of the cone the temperature becomes less than T_{wp}, in contrast with the flow over the impermeable body.

According to the above notation, Fig. 2 shows the dynamics of surface temperature variation at various sections along the generator (lines 1-3 for ξ = 0.2; 0.67; 4) for the laminar flow regime (a) and laminar transition to turbulent flow in the boundary layer (b). It can be seen that for the conducting material there is a considerable extension of the time for the flow process to come to a stationary regime, and this time depends on the heat flux along the generator, the wall thickness, and the thermophysical properties of the material, and it decreases very strongly for porous blunting in the presence of gas blowing.

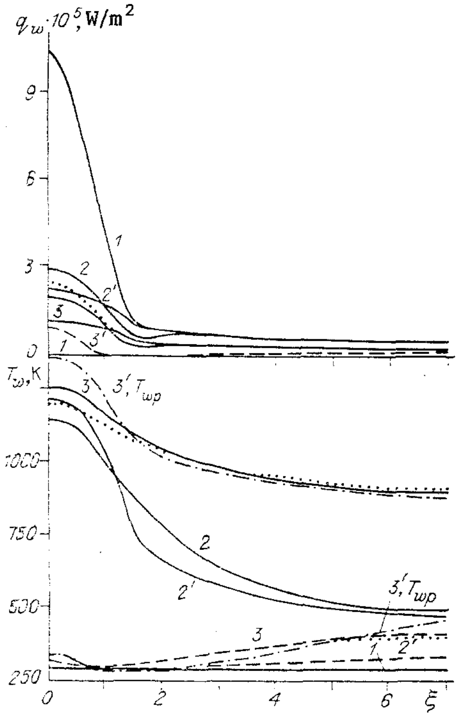

Fig. 1

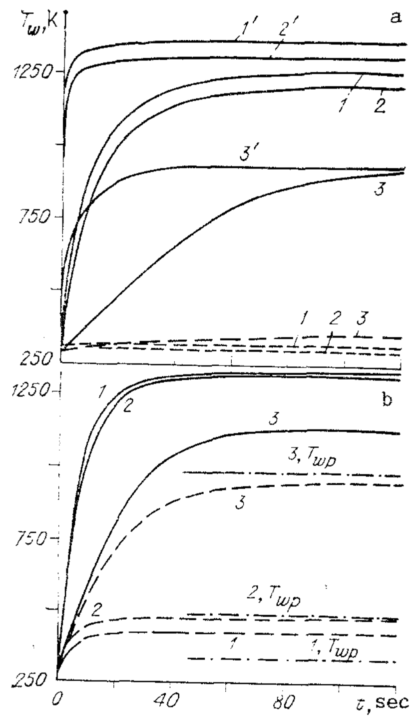

Fig. 2

There is interest in how the heat transfer coefficients behave in the wall heating. Figure 3 shows the computed results of the coupled problem in the form of the dependence

$$\frac{\mathrm{St}}{\mathrm{St}_i} = \frac{q_w(\xi)\,[T_{e0} - T_i]}{[T_{e0} - T_w(\xi)]\,q_{wi}(\xi)},$$

this being the ratio of the heat transfer coefficients at a fixed section ξ to the value at time zero for an isothermal surface, on the process time and the surface temperature (Fig. 3a, b). Figure 3a shows data obtained for $\xi = 1.4;\ 1.7;\ 4$ for a conducting wall (curves 1-3), and a nonconducting material (1'-3'). The heat transfer coefficients or the Stanton numbers are monotonic, which agrees with the analytical solutions [4, 11], which have shown a dependence of St on the temperature factor and the quantity $\frac{1}{(T_{e0} - T_w)}\frac{\partial T_w}{\partial \xi}$. For negative values of $\partial T_w/\partial \xi$, typical of the geometry considered, St increases at times near the initial value, when the surface becomes nonisothermal, and then as $\partial T_w/\partial \xi$ decreases and the temperature factor increases, St begins to decrease. What has been said above is also illustrated by the behavior of $\mathrm{St}/\mathrm{St}_i(\theta_w)$ for $\xi = 1.4$ and 4. It can be seen that for thin walls the nonmonotonic dependence of heat transfer coefficient on surface temperature also occurs on the conical surface. This behavior of $\alpha/c_p = q_w/(H_{e0} - h_w)$ must be accounted for in solving the heating problem in a different formulation with boundary conditions of the third kind, since for the known dependences $\alpha/c_p(T_w)$ decreases monotonically with increase of surface temperature, which will lead to a decrease of heat flux and wall temperature on the side of the body. In this case for threshold values from the gas phase we can use equations [4, 11] constructed for the general case of nonisothermal surfaces.

We now consider further the case of turbulent flow in the boundary layer. Figure 4 shows the dependences for $q_w(\xi)$, $T_w(\xi)$ at t = 0,30, 120 sec for a conducting wall (curves 1-3) and a nonconducting wall (lines 1 and 3' for t = 0, 60 sec). The other symbols and the governing parameters coincide with those for Fig. 1. As was true for laminar flow, for the nonconducting wall curves 3' coincide with the values of $T_{wp}(\xi)$, and from Figs. 1 and 4 one can see a weaker decrease of maximum surface temperature due to flow of heat for the turbulent regime for $(\rho v)_w = 0$, due to decrease of surface temperature gradients. However, with blowing of coolant, using effects of heat flow in the material, one can noticeably decrease the wall temperature in the thermal curtain region behind the blowing section. The use of heat conducting material leads to equilibration and monotonic behavior of the temperature of the porous spherical wall, and the temperature distribution can be changed by choosing the wall thickness (broken lines for $L/R_N = 0.085$). As follows from the calculations, for a nonconducting material on the permeable blunted sphere the steady-state regime is established in

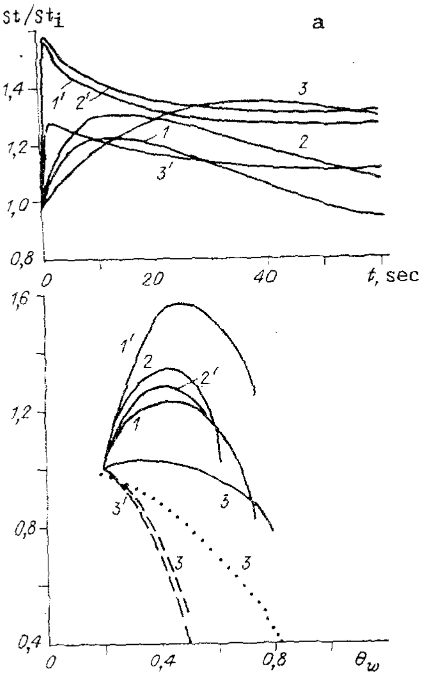

Fig. 3

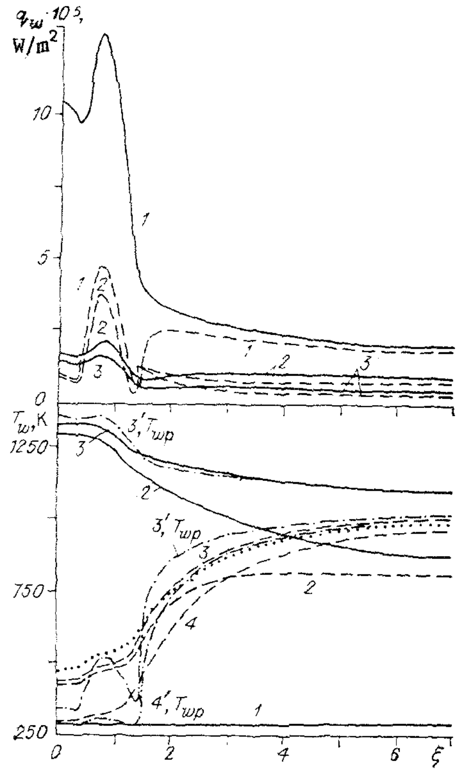

Fig. 4

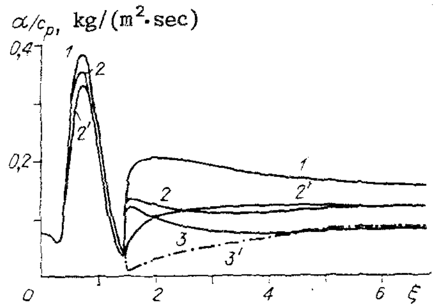

Fig. 5

the first second and the surface temperature equals T_{wp}, which coincides also with the analytical solution, derived from the balance condition at the surface, Eq. (2.2), for the given heat transfer coefficient from the gas phase. The behavior of the surface temperature of a conducting wall on time with gas blowing is shown in Fig. 2b, which also shows the steady value T_{wp} at the corresponding sections with respect to ξ. From Fig. 2b one can also track the change of monotonic behavior of $T_w(\xi)$ for a conducting wall at different times: from a decreasing function for $(\rho v)_w = 0$ to an increasing one in the presence of blowing.

For the spherically blunted surface isothermal and different blowing intensities we developed the relationship in the form of the widely used dependence of $\alpha/c_p/(\alpha/c_p)^0$ on $(\rho v)_w/(\alpha/c_p)^0$, where $(\alpha/c_p)^0$ corresponds to the impermeable surface, for various values of Re. It has been shown that if for the experimental conditions of [10] with Re = $3.872 \cdot 10^6$ the theoretical and experimental results coincide for various values of ξ in the turbulent flow region [7] and is described by the formula suggested in [12] $\frac{\alpha}{c_p}\Big/\left(\frac{\alpha}{c_p}\right)^0 = \exp\left[-0.37\frac{(\rho v)_w}{(\alpha/c_p)^0}\right]$, then, with decrease of Re for the maximum heat flux region near the sonic line there is a noticeable decrease of the curves of relative heat transfer coefficient or of relative heat flux as a function of the blowing parameter $(\rho v)_w/(\alpha/c_p)^0$. Thus, with decrease of Re the effectiveness of blowing, linked to decrease of heat flux, increases, which should be taken into account in evaluating heat flux to a permeable surface with turbulent flow conditions.

For gas blowing from a surface Fig. 5 shows the distribution of heat transfer coefficients along generators at the same times as for Fig. 4, and the dot-dash curve was obtained for the equilibrium surface temperature T_{wp}. It can be seen that if on the permeable spherically blunted surface α/c_p varies insignificantly for the computed temperature distributions of a sphere, then in the curtain zone the heat transfer coefficient is decreased very stongly, and immediately behind the blowing section there is a different qualitative behavior due to the distribution $T_w(\xi)$ for different wall materials. For the turbulent flow regime Fig. 3b shows the ratio St/St_i at the section $\xi = 2$ (curves 3 and 3') without and with blowing to the blunted surface (solid and broken curves). It can be seen that for $(\rho v)_w = 0$ the curve has a weak maximum, due to the nonisothermal behavior of the wall temperature, and agrees qualitatively with values computed for laminar flow. With gas blowing the dependence $St/St_i(\theta_w)$ is monotonically decreasing for different wall materials. It is important to note that the computed behavior of the wall temperature in the curtain zone leads to very strong differences in heat transfer coefficient compared with the case of an isothermal surface. For instance, the dotted curve 3 (Fig. 3b) illustrates the behavior of $St/St_i(\theta_w)$ with parametric variation of the surface temperature $T_w(\xi)$ = const and may exceed the results of solving the coupled problem by more than a factor of 2. Thus, compared with the isothermal wall case, in solving the heating problem due to choice of wall thickness and wall material of the conical section one can obtain added substantial gain in reducing heat flux in the curtain zone due to the formation of $T_w(\xi)$ and decrease of the heat transfer coefficient. These conclusions conform with the analysis conducted on the influence of an isothermal wall temperature [11, 13], since the heat transfer coefficients decrease for a positive value of $\frac{1}{(T_{e0}-T_w)}\frac{\partial T_w}{\partial \xi}$, typical of the thermal curtain section.

As one would expect an increase of coolant gas flow rate decreases the temperature of the blunted and conical sections of the body. Figure 4 shows the distribution along the generators of the equilibrium radiative temperature T_{wp} (curve 4') and the temperature T_w (line 4) corresponding to stationary conditions at t = 100 sec in flow over a conducting wall, for a mass flow rate of $(\rho v)_w = 3.25$ kg/(m^2·sec), with the other governing parameters having their previous values. For the nonconducting spherically blunted wall the maximum temperature reaches 311 K, and in the thermal curtain zone the greatest decrease of T_w in choosing a conducting material is more than 100 K. We note that for the given values of $(\rho v)_w$ the total mass flow rate of coolant gas is 0.048 kg/sec. This establishes that one can achieve thermal protection by blowing for the process times considered up to the end of the steady-state conditions.

Thus, in this paper we have illustrated the influence of heat flow and surface gas blowing on the heat transfer characteristics, which can be used when interpreting data of an aerodynamic experiment. We note that the conclusion that one must account for heat flow along the model surface when the heat flux depends appreciably on the longitudinal coordinate was reached in [14], where an approach was suggested, based on analysis of experimental results for computing the influence of heat flow, and formulas were obtained for evaluating the errors due to neglecting this. The question of computing heat flow is relevant in creating heat flux sensors with long measurement time, allowing reduced cost of tests by conducting the experiments under varying conditions. One source of error in determining heat flux in this case also is heat flux along the wall, which one should account for in developing the sensor structure, the nominal model, and the method of recovering the surface heat flux. As was shown above, these questions, relating to accounting for heat flux along the model, the nonisothermal nature of the model surface, and the influence of these factors on the heat transfer coefficients can be resolved by solving the problem in the coupled formulation.

LITERATURE CITED

1. V. A. Bashkin and S. M. Reshet'ko, "The maximum temperature of a blunted region, accounting for heat conduction," Uchen. Zap. Tsentr. Aero. Gid. Ints., 20, No. 5 (1989).
2. V. A. Bashkin and S. M. Reshet'ko, "Temperature regimes over blunted wedges and cones in supersonic flow, accounting for heat conduction of the wall material," Uchen. Zap. Tsentr. Aero. Gidr. Inst., 21, No. 4 (1990).
3. A. V. Lykov, Heat and Mass Transfer: Handbook [in Russian], Énergiya, Moscow (1972).
4. V. I. Zinchenko, and E. I. Putyatina, "Solution of the coupled heat transfer problem in flow over different shapes," Prikl. Mekh. Tekh. Fiz., No. 2 (1986).

5. T. Cebeci, "Behavior of turbulent flow near a porous wall with pressure gradient," AIAA J., 8, No. 12 (1970).
6. K. K. Chen and N. A. Thyson, "Extension of Emmons' spot theory to flows over blunt bodies," AIAA J., 9, No. 5(1971).
7. A. V. Bureev and V. I. Zinchenko, "Computation of flow over a spherically blunted cone for various flow regimes in the shock layer and gas blowing from the surface," Prikl. Mekh. Tekh. Fiz., No. 2 (1991).
8. A. M. Prishin, V. N. Bertsun, and V. I. Zinchenko, An Iteration-Interpolation Method and its Application [in Russian], TGU, Tomsk (1981).
9. N. N. Yanenko, Method of Fractional Steps for Solving Multi-Dimensional Problems of Mathematical Physics [in Russian], Nauka, Novosibirsk (1987).
10. R. H. Feldhuhm, "Heat transfer from a turbulent boundary layer on a porous hemisphere," AIAA Paper No. 119, NY (1976).
11. V. I. Zinchenko and O. P. Fedorova, "Numerical investigation of the three-dimensional laminar boundary layer accounting for coupled heat transfer," Prikl. Mekh. Tekh. Fiz., No. 2 (1988).
12. Yu. V. Polezhaev and F. B. Yurevich, Thermal Protection [in Russian], Énergiya, Moscow (1976).
13. V. I. Zinchenko and O. P. Fedorova, "Investigation of the three-dimensional turbulent boundary layer accounting for coupled heat transfer," Prikl. Mekh. Tekh. Fiz., No. 3 (1989).
14. V. N. Brazhko, N. A. Kovaleva, and G. I. Maikapar, "A method of measuring heat flux using thermal-indicator coatings," Uchen. Zap., Tsentr. Aero. Gidr. Inst., 20, No. 1 (1989).